


Original Article

Reproducibility of the NanoString 22-gene molecular subgroup assay for improved prognostic prediction of medulloblastoma

Letícia F. Leal,^{1*} Adriane F. Evangelista,^{1*} Flávia E. de Paula,^{2*} Gisele Caravina Almeida,³ Adriana C. Carloni,¹ Fabiano Saggioro,⁴ João N. Stavale,⁵ Suzana M.F. Malheiros,⁵ Bruna Mançano,⁶ Marco A. de Oliveira,⁷ Betty Luu,⁸ Luciano Neder,^{1,3} Michael D. Taylor⁸ and Rui M. Reis^{1,2,9,10} 

¹Molecular Oncology Research Center, ²Molecular Diagnostic Laboratory, ³Department of Pathology, ⁶Children and Young Adult's Cancer Hospital, ⁷Statistics Unity, Barretos Cancer Hospital, Barretos, ⁴Department of Pathology, Ribeirao Preto Medical School, University of São Paulo, Ribeirao Preto, ⁵Department of Pathology, Universidade Federal de São Paulo, São Paulo, Brazil, ⁸Hospital for Sick Children, University of Toronto, Toronto, Ontario, Canada, ⁹Life and Health Sciences Research Institute (ICVS), Health Sciences School, University of Minho, Braga and ¹⁰ICVS/3B's-PT Government Associate Laboratory, Braga/Guimarães, Portugal

Medulloblastoma is the most frequent malignant brain tumor in children. Four medulloblastoma molecular subgroups, MB_{SHH}, MB_{WNT}, MB_{GRP3} and MB_{GRP4}, have been identified by integrated high-throughput platforms. Recently, a 22-gene panel NanoString-based assay was developed for medulloblastoma molecular subgrouping, but the robustness of this assay has not been widely evaluated. Mutations in the gene for human telomerase reverse transcriptase (*hTERT*) have been found in medulloblastomas and are associated with distinct molecular subtypes. This study aimed to implement the 22-gene panel in a Brazilian context, and to associate the molecular profile with patients' clinical-pathological features. Formalin-fixed, paraffin-embedded (FFPE) medulloblastoma samples ($n = 104$) from three Brazilian centers were evaluated. Expression profiling of the 22-gene panel was performed by NanoString and a Canadian series ($n = 240$) was applied for training phase. *hTERT* mutations were analyzed by PCR followed by direct Sanger sequencing and the molecular profile was associated with patients' clinicopathological features. Overall, 65% of the patients were male, average age at diagnosis was 18 years and 7% of the patients presented metastasis at diagnosis. The molecular

classification was attained in 100% of the cases, with the following frequencies: MB_{SHH} ($n = 51$), MB_{WNT} ($n = 19$), MB_{GRP4} ($n = 19$) and MB_{GRP3} ($n = 15$). The MB_{SHH} and MB_{GRP3} subgroups were associated with older and younger patients, respectively. The MB_{GRP4} subgroup exhibited the lowest 5-year cancer-specific overall survival (OS), yet in the multivariate analysis, only metastasis at diagnosis and surgical resection were associated with OS. *hTERT* mutations were detected in 29% of the cases and were associated with older patients, increased *hTERT* expression and MB_{SHH} subgroup. The 22-gene panel provides a reproducible assay for molecular subgrouping of medulloblastoma FFPE samples in a routine setting and is well-suited for future clinical trials.

Key words: *hTERT*, medulloblastoma, molecular subgroups, NanoString.

INTRODUCTION

Medulloblastoma is the most frequent malignant brain tumor in children, accounting for approximately 20% of all pediatric intracranial tumors.^{1,2} Recent estimates of the occurrence of central nervous system tumors, such as medulloblastoma, suggest they represent about 2.5% of the newly diagnosed cases of pediatric neoplasms in Brazil.³ In adults, medulloblastomas are less common, with a peak of incidence between 20 and 35 years old.⁴ Advances in the treatment of medulloblastoma have improved survival rates over the last few decades. However, the disease outcome remains very poor, with both 5-year overall and

Correspondence: Rui M. Reis, PhD, Molecular Oncology Research Center, Barretos Cancer Hospital, Rua Antenor Duarte Vilela, 1331; CEP 14784 400, Barretos, S. Paulo, Brazil. Email: ruireis.hcb@gmail.com

*LFL, AFE and FEP equally contributed to this work.

Received 06 April 2018; Revised 22 June 2018; Accepted 25 July 2018; published online 28 August 2018.

event-free survivals for high-risk patients being about 25–44%.^{5–7}

Histologically, medulloblastomas can be classified as classic, the most common subtype (70%), followed by the desmoplastic (10–20%), anaplastic/large-cell subtype (5–10%) and extensive nodularity subtype (5–10%).^{5,8} The major prognostic factors are histology, age at diagnosis, presence of metastatic disease, and the extent of tumor volume at resection.^{9,10} Younger medulloblastoma patients, who have evidence of metastasis at diagnosis, residual disease after surgery or large cells/anaplastic histology, are associated with an unfavorable prognosis.^{9,11,12} Until recently, these clinical and pathological prognostic factors were used for defining overall disease risk, but newer combinations of clinical, pathological and molecular prognostic markers are providing a more accurate disease risk stratification.¹³

Medulloblastomas can be molecularly classified based on specific genomic and genetic features.^{14–16} Gene expression analysis using large cohorts of medulloblastomas has identified four molecular subgroups of medulloblastoma, namely WNT (MB_{WNT}), SHH (MB_{SHH}), group 3 (MB_{GRP3}) and group 4 (MB_{GRP4}).^{14,16,17} Moreover, this molecular classification correlates with several clinical-pathological features, such as patient prognosis, histology and age at diagnosis.^{10,17} The MB_{WNT} subgroup has a better prognosis, whereas MB_{GRP3} patients present with a poor prognosis.¹⁸ MB_{WNT} medulloblastomas can occur at all ages, but are infrequently seen in infants and are more common in children. The MB_{GRP4} subgroup is also more frequent in children, but it can also be seen in both infant and adult medulloblastoma. MB_{GRP3} tumors are frequent in infants and children, but are rare in adults, whereas MB_{SHH} subgroups are very frequent in both infants and adults.^{10,17,19} Thus, subgroup analysis using gene expression signatures is providing clinicians with a new tool for improved management of medulloblastoma patients.

In addition to molecular signatures, gene alterations such as mutations in the promotor region of the gene for human telomerase reverse transcriptase (*hTERT*) have been described in about 20% of medulloblastomas, and they correlate with a worse prognosis.²⁰ Furthermore, the presence of *hTERT* promoter mutations is associated with a higher expression of *hTERT* gene in medulloblastomas, especially in non-infant MB_{SHH}.^{20–22}

The nCounter[®] system (NanoString Technologies, Seattle, WA, USA) is an automated high-throughput platform designed to evaluate mRNA expression. The mRNA expression levels are directly measured with a high sensitivity in a single multiplexed hybridization reaction.²³ The nCounter[®] platform is particularly well-suited for expression analysis of formalin-fixed, paraffin-embedded (FFPE) samples, as the quality of these samples may be highly

variable, producing low yields of highly degraded mRNA.²⁴ Furthermore, the nCounter[®] technology does not require further validation, since it does not require enzymatic reactions, it generates reproducible results.²³ Northcott and colleagues constructed a 22-gene panel that could accurately distinguish medulloblastoma molecular subgroups using the nCounter[®] platform. The 22 genes they selected have differential expressions associated with each molecular subgroup.²⁵

The aim of the present study was to implement the 22-gene panel for molecular classification of medulloblastomas from FFPE blocks using the nCounter[®] technology in a Brazilian population, and to associate the molecular subgroups with the *hTERT* mutational status and clinical-pathological features of our cohort.

MATERIAL AND METHODS

Patients

Brazilian cases

A series of 104 patients with medulloblastoma were retrieved between 1995 and 2017 from three Brazilian reference centers: the Barretos Cancer Hospital (BCH), Ribeirao Preto Medical School of University of Sao Paulo (FMRP-USP); and Universidade Federal de São Paulo (UNIFESP). In two cases (patients #87 and #98; Table S1), we assessed both primary and metastatic tissues. The histologic diagnoses of all cases were reviewed by two expert neuropathologists in accordance with revised 2016 WHO classification, which has histologically defined medulloblastomas as classic, desmoplastic/nodular, extensive nodularity or large cell/anaplastic.²⁶ The summary of clinical-pathological and molecular features is presented in the Table S1. This study was approved by the local ethics committee (#478/2011).

Canadian series

The molecular data of a series comprising 240 medulloblastomas from the Hospital for Sick Children, University of Toronto, Canada, was kindly provided by Dr. Michael Taylor, and were employed for class prediction.²⁵

RNA isolation

RNA was isolated from three to five 10- μ m-thick sections using RNeasy Mini kit (Qiagen, Venlo, Netherlands) following the manufacturer's instructions. Briefly, following deparaffinization steps, unstained slides were scraped upon a tumor area demarcated on a HE slide. All specimens were submitted to protease digestion followed by nucleic acid isolation followed by DNase digestion and sample elution. RNA concentrations were assessed by spectrophotometry (NanoDrop; Thermo Fisher Scientific,

Waltham, MA, USA) and a subset of samples were also evaluated by BioAnalyzer (Agilent Technologies, Inc., Santa Clara, CA, USA).

The nCounter[®] system (NanoString)

The medulloblastoma panel was carried out using the *NanoString nCounter Elements*[™]. The custom CodeSet was designed using characteristic genes for each medulloblastoma subgroup as previously employed: MB_{SHH} – *PDLIM3*, *EYAI*, *HHIP*, *ATOHI*, *SFRP1*; MB_{WNT} – *WIFI*, *TNC*, *GAD1*, *DKK2*, *EMX2*; MB_{GRP3} – *IMPG2*, *GABRA5*, *EGFL11*, *NRL*, *MAB21L2*, *NPR3*; MB_{GRP4} – *KCNA1*, *EOMES*, *KHDRBS2*, *RBM24*, *UNC5D*, *OASI* and three housekeeping genes (*ACTB*, *GAPDH* and *LDHA*).²⁵ In addition, 11 other cancer genes including *hTERT* gene were added to the gene panel CodeSet used in this study. The expression analysis of the *hTERT* gene was performed for the present study and the analyses of the other 10 genes will be further reported (manuscript in preparation). All procedures regarding sample preparation, hybridization, detection and scanning were performed according to the manufacturer's instructions (NanoString Technologies, Seattle, WA, USA).

The custom probes (A and B) were designed by IDT (IDT Technologies), containing 35–50 base pairs each and probes were diluted to a final concentration of 0.6 nmol/L (probe A) and 3.0 nmol/L (probe B) to create the working probe pools. A total amount of 100–300 ng RNA was hybridized with probe pools, hybridization buffer and TagSet reagents and incubated at 67 °C for 21 h. Then, samples were loaded to the nCounter[®] PrepStation (NanoString), which automatically performs purification steps and cartridge preparation. Finally, the cartridges containing immobilized reporter complexes were transferred to nCounter[®] Digital Analyzer (NanoString), a high-resolution setting, which captures up to 280 fields of view (FOVs) per sample providing all gene counts.

DNA isolation and *hTERT* mutational analysis

DNA was isolated from three to five sections each 10 μm thick using QIAmp DNA Mini kit (QIAGEN) as previously reported.²⁰ DNA concentrations were assessed by spectrophotometry (NanoDrop).

hTERT promoter hotspot mutations (–124 bp G > A and –146 bp G > A) were screened by PCR followed by Sanger sequencing as previously described.^{20,27} All samples with mutations were confirmed at least twice.

Data analysis

Reporter probe counts were captured by nCounter[®] Digital Analyzer and raw data was collected and pre-processed by nSolver[™] Analysis Software v3.0 (NanoString). For data normalization, NanoStringNorm package was employed (version 18 November, 2015; <http://cran.r-project.org/web/packages/NanoStringNorm>).²⁸ The normalization method basically consists of four major corrections, which are probe-level background correction, code-count normalization, background correction and sample content normalization by housekeeping genes. The NanoStringNorm package uncovers potential batch-effects, identifies background artifacts and assesses negative/positive controls. Each parameter for all normalizations is associated with plots and all results, diagnostics and expression values were outputted for statistical analyses, heatmaps design and use in class prediction methodologies.

For class prediction analysis of the Brazilian series ($n = 104$), the Canadian series ($n = 240$) was employed to establish a prediction dataset, since all samples had been previously classified for medulloblastoma molecular subgroups.²⁵ Raw data from all samples (Brazilian and Canadian series) were normalized and the gene expression values were defined. Normalized data were input for class prediction analysis using the Prediction Analysis for Microarrays (PAM) algorithm.²⁹ PAM is a statistical technique for class prediction from gene expression data using nearest shrunken centroids. Class prediction was performed using a machine learning method following these analytical phases: (i) training phase: data from Canadian series were considered for input by pairing with the expected output to train our model employing the PAM algorithm; (ii) validation phase: data from the Brazilian series employing the heatmap clustering as gold-standard were used for initial classification of medulloblastoma molecular subgroups applying the PAM method; (iii) test phase: application of our model to the Brazilian series for class prediction and probability results.

For analysis of *hTERT* mRNA expression, Mann-Whitney test was applied for comparing wild-type and *hTERT* mutated cases. Survival analysis was carried out by Kaplan–Meier curves, which were compared by the log-rank test. For disease-specific overall survival (OS), patients who were lost to follow-up were censored considering their last follow-up visit, and patients who died due to external causes or surgical complications were censored considering death date as the last data entry. For all analyses, cancer-specific death was considered as the unfavorable event.

For pre-processing and normalization, statistical analyses, graph constructions, heatmap designs and class

prediction, the KNIME v.3.2.0 software (KNIME GmbH, Konstanz, Germany) was employed in the R environment (R Foundation, Vienna, Austria). For survival analysis, the IBM SPSS Statistics for Windows version 21.0 (IBM, Armonk, NY, USA) and GraphPad Prism version 6.0 (GraphPad Software, San Diego, CA, USA) were employed. A Cox multivariate analysis considering age and gender as confounders was performed for disease-specific OS analysis. The level of significance for all analyses was 5%.

RESULTS

Clinicopathological features of Brazilian patients

We evaluated 104 tumors from patients diagnosed with medulloblastoma (Table 1; Table S1). Thirty-six (35%) patients were female and 67 (65%) were male (data were unavailable from one patient). The average age at diagnosis was 18 years old (range, 2–56 years), with 11 patients \leq 4 years old, 55 cases between 5 and 19 years old, and 37 more than 20 years old (no available information for one patient). Clinical findings showed that 93% of the patients (92/99) did not have metastasis at diagnosis, whereas 7% (7/99) of the patients presented metastasis at diagnosis (data were not available for five cases). Additionally, 63% of the patients (59/94) underwent total surgical resection and 37% (35/94) partial surgical resection. For two patients, surgery was not performed and they were subjected to biopsy only (data were not available for eight cases). Histologic classification showed that 57% (59/104) had classic histology, 24% (25/104) desmoplastic/nodular histologic features, 4% (4/104) anaplastic/large cells, and 12% (13/104) extensive nodularity, and 1% (1/104) mixed histology. One case was not clearly defined and one case presented inconclusive histological features (Table 1; Table S1).

Overall survival was associated with metastasis at diagnosis ($P = 0.04$) and surgical resection ($P = 0.001$; Table S2).

Classification of medulloblastoma molecular subgroups

We obtained conclusive results from all 106 FFPE samples that comprised 104 primary samples and two metastatic samples. We initially performed an unsupervised clustering to generate heatmaps (Figure S1). The Canadian series provided the known class predictions for comparison to the subgroup findings from the Brazilian cohort.²⁵ Following normalization of raw data from both series (Canadian series combined with the Brazilian series; Figure S1), the PAM method was applied for class prediction. Employing a machine learning approach, we successfully classified all medulloblastoma samples according to molecular subgroups (Figs 1, 2A). The probability of each subgroup for all samples and the highest probability index for specific molecular subgroups was considered for the final classification. Most samples in each subgroup presented a probability rate higher than 90%. Therefore, the final proportions for classification of the Brazilian medulloblastoma subgroups was 49% MB_{SHH} ($n = 51$), 18% MB_{WNT} ($n = 19$), 14% MB_{GRP3} ($n = 15$) and 18% MB_{GRP4} ($n = 19$) (Figs 1, 2A; Table 1).

Interestingly, for the two patients (patients #87 and #98; Table S1) in which both primary and metastatic tissue could be evaluated, each pair exhibited the same molecular profile (MB_{SHH}).

Association of molecular subgroups with clinicopathological features

Clinical and molecular features of the molecular subgroup are summarized in Table 1 and described in detail in Table S1. Older age patients were strongly associated with the MB_{SHH} subgroup and younger patients with MB_{GRP3} ($P < 0.0001$; Table 1). No association by age category (< 4 , 5–19 and > 20 years) and disease outcome was observed ($P = 0.1$). The female gender was strongly associated with MB_{WNT} ($P < 0.0001$; Table 1).

Table 1 Clinical and molecular characteristics of Brazilian cohort according to the medulloblastoma molecular subgroups

MB molecular subgroup	n	Average age (range)	F/M ratio	Histology [†]				hTERT mutation	
				Classic	Anaplastic/large cells	Extensive nodularity	Nodular/desmoplastic	%	Mutated cases
MB _{SHH}	51	24 years (2–56 years)	1:2.4	20	2	3	24	77	17
MB _{WNT}	19	13 years (4–27 years)	3.75:1	13	0	5	0	9	2
MB _{GRP3}	15	8 years (4–17 years)	1:6.5	10	2	2	1	9	2
MB _{GRP4}	19	13 years (4–32 years)	1:3.75	16	0	3	0	5	1
All	104	18 years (2–56 years)	1:1.6	59	4	13	25	29	22/76

[†]One case from MB_{SHH} was classified as Mixed, one case was not possible to classify, and one case no data were available. MB, medulloblastoma; n, number of cases; F, female; M, male.

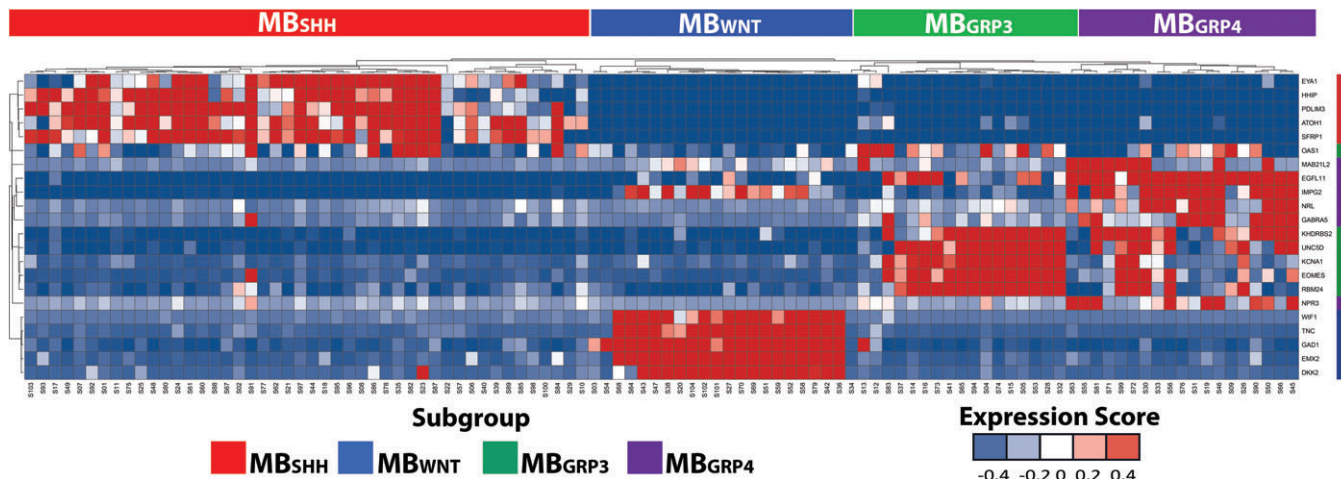


Fig. 1 Heatmap clustering of the Brazilian series ($n = 104$). On the top and on the right side, each colored column represents a medulloblastoma subgroup: MB_{SHH}, red; MB_{WNT}, blue; MB_{GRP4}, purple; MB_{GRP3}, green. Lower right color squares: gene expression scaling from dark blue (-0.4) to dark red ($+0.4$), with red: increased gene expression; blue: decreased gene expression; white: no differential expression.

Univariate analysis indicated a trend of association between disease-specific OS and medulloblastoma molecular subgroup (log-rank test: $P = 0.07$; Fig. 2B; Table S2). The highest 5-year disease-specific OS was observed for the MB_{WNT} (100%) subgroup, followed by MB_{GRP3} (73%), MB_{SHH} (64%) and MB_{GRP4} (63%).

Multivariate analysis showed a higher hazard ratio (HR) for patients who underwent partial surgical resection (HR = 3.73, $P = 0.006$; Table 2), but no increased HR was observed for age, gender, metastasis at diagnosis, or for molecular subgroup (Table 2).

hTERT mutational status

Hotspot *hTERT* promoter mutations (-124 bp G > A and -146 bp G > A) were successfully sequenced in 73.1% (76/104) of tumors. Of these, 29% (22/76) of the cases were mutated (Fig. 3A), with 82% (18/22) harboring the -124 bp G > A mutation and 18% (4/22) the -146 bp G > A mutation. The frequency of *hTERT* mutations was significantly higher in the MB_{SHH} subgroup (77%), than in MB_{WNT} (9%), MB_{GRP3} (9%), and MB_{GRP4} (5%) ($p = 0.002$; Table 1; Table S1). The distribution of *hTERT* mutation was associated with older age as follows: 4.5% (1/22) of mutated cases in patients ≤ 4 years old, 36.4% (8/22) of mutated cases between 5 and 19 years old, and 59.1% (13/22) of mutated cases in patients more than 20 years old ($P = 0.002$). We extended our analysis to determine whether *hTERT* mutational status correlated with *hTERT* gene expression assessed in the NanoString gene panel, and we found that *hTERT* mutated tumors exhibited a significantly increased *hTERT* expression ($P = 0.03$; Fig. 3B). Since most of the *hTERT* mutated cases belonged to the

MB_{SHH} subgroup, we also evaluated whether *hTERT* mutational status and *hTERT* expression correlated with OS in this specific subgroup, but no association was observed ($P = 0.41$ and 0.31 , respectively). Moreover, neither *hTERT* mutational status nor *hTERT* expression was associated with OS ($P = 0.34$ and $P = 0.72$, respectively; Fig. 3C, D).

DISCUSSION

Four major medulloblastoma molecular subgroups (MB_{WNT}, MB_{SHH}, MB_{GRP3}, MB_{GRP4}) have been described based on specific molecular characteristics, such as mutations and differential expressions of key genes.^{14–17,30} The assignment of medulloblastoma molecular subgroups plays an important role in patient prognostication,^{30,31} and may also be crucial in the design of potential targeted therapies. Herein, we have successfully implemented an effective approach for medulloblastoma molecular subgrouping using FFPE from 104 cases from Brazilian health centers. Additionally, we reported the main clinical and molecular characteristics for each molecular subgroup.

The molecular pathogenesis of medulloblastomas has been partially elucidated by microarray expression profiling and, until recently, this high-throughput technique was the best approach in determining medulloblastoma molecular subgroups.^{14,15,30} However, these earlier platforms required large amounts of high-quality RNA, presented a high variability and are expensive, limiting their application as a routine diagnostic approach. Since there is no current gold-standard method for medulloblastoma molecular subgrouping, the implementation of a robust and inexpensive method is urgently needed. For this reason,

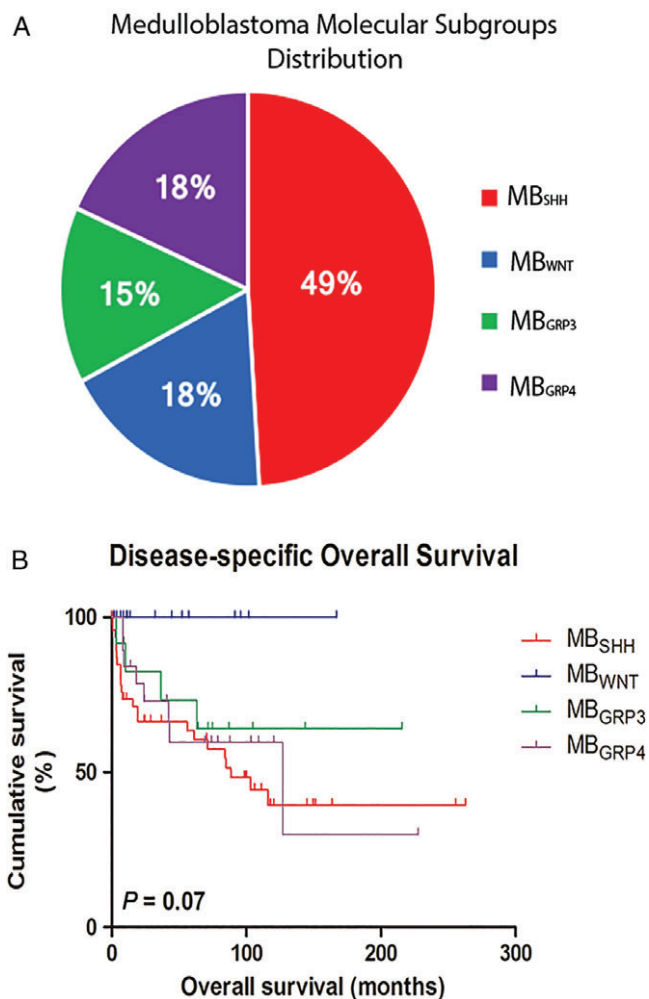


Fig. 2 (A) Medulloblastoma molecular subgroup distributions. Data derived from the Brazilian series ($n = 104$). In this circle chart each colored segment represents a medulloblastoma subgroup: MB_{SHH} , red; MB_{WNT} , blue; MB_{GRP4} , purple; MB_{GRP3} , green. (B) Disease-specific overall survival. Kaplan–Meier curves of overall survival data derived from 99 available patients in the Brazilian series and expressed according to the medulloblastoma molecular subgroups. Cumulative survival as a percentage is shown on the Y-axis and overall survival in months on the X-axis (log-rank test: $P = 0.07$). Live patients, patients who were lost follow up or patients who died due to non-cancer-related causes or surgical complications were censored.

Dr. Taylor's group developed the 22-gene panel for the assignment of medulloblastoma molecular subgroups employing an innovative platform (nCounter® system; NanoString) applied to FFPE samples, which are routinely collected for histopathological analysis.²⁵

For actual assignment of the medulloblastoma molecular subgroups based on high-throughput gene expression, it is necessary to employ class prediction analysis. Several algorithms were previously tested by Dr. Taylor's group and the PAM method presented the best scoring index with the lowest misclassification rates compared with other statistical approaches.²⁵ This method is faster and can

Table 2 Multivariate proportional hazard analysis on the disease outcome (disease-specific overall survival) of the molecular and clinical characteristics

Variables	<i>n</i>	HR (95% CI)	<i>P</i> -value
Age			
Age < 4 years	8	Ref.	Ref.
Age group 5–19 years 2	40	0.53 (0.16–1.76)	0.30
Age group ≥ 20 years 3	20	0.60 (0.16–2.28)	0.45
Gender			
Male	61	Ref.	Ref.
Female	20	0.97 (0.45–2.12)	0.94
Surgical resection			
Total surgical resection	42	Ref.	Ref.
Partial surgical resection	26	3.73 (1.47–9.47)	0.006
Metastasis at diagnosis			
Absence of metastasis at diagnosis	63	Ref.	Ref.
Presence of metastasis at diagnosis	5	0.87 (0.16–4.77)	0.88
<i>hTERT</i> mutational status			
<i>hTERT</i> wild-type	48	Ref.	Ref.
<i>hTERT</i> mutated	20	1.76 (0.72–4.32)	0.22
Molecular subgroup			
MB_{SHH}	31	Ref.	Ref.
MB_{GRP3}	11	0.91 (0.25–3.26)	0.88
MB_{GRP4}	17	0.88 (0.25–3.15)	0.84
MB_{WNT}	9	0.00 ()	0.97

Reference categories: Gender male; molecular subgroup MB_{SHH} . † MB_{WNT} was not possible to estimate because no event (death) was observed for this subgroup (disease-specific overall survival = 100%). *P*-values are from Cox proportional hazards analysis. HR, hazard ratio; 95% CI, 95% confidence interval; Ref, reference category.

improve accuracy by reducing the effect of intrinsic noise from highly expressed genes, providing easily interpretable results for biologists and clinicians.²⁹ For this reason, the PAM method was employed for class prediction in the present study. The gene expression analysis employing the nCounter® technology using the 22-gene panel together with the PAM method for class prediction could classify according to molecular subgroups all medulloblastoma samples analyzed. We also observed the concordance of molecular subgroups in paired primary and metastatic tissues in two patients in accordance with previous data.³² In our series, the majority of cases (49%) were classified in the MB_{SHH} subgroup, followed by MB_{WNT} (18%), MB_{GRP4} (18%) and MB_{GRP3} (14%). These frequencies differ slightly from the reported series, that reported higher frequencies of MB_{GRP3} (20–26%) and MB_{GRP4} (35–37%), which could be explained, at least in part, by the older age (18 years average) of our cohort in comparison with other studies.^{25,31}

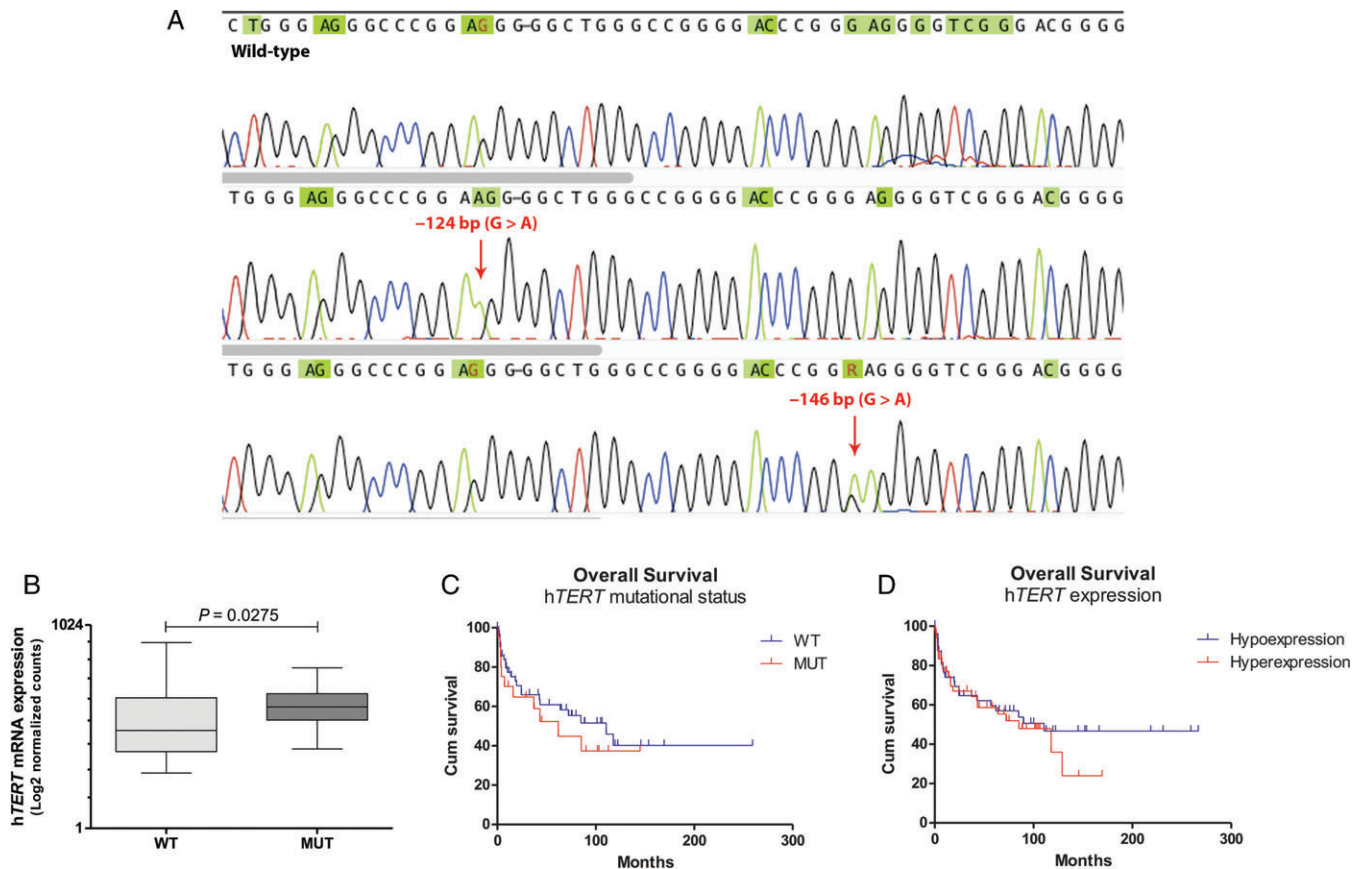


Fig. 3 Analysis of mutation and expression status of *hTERT*. (A) Nucleotide sequencing of *hTERT* promoter region showing hotspot promoter mutations (-124 bp G > A and -146 bp G > A) identified in medulloblastoma samples. (B) *hTERT* mRNA expression in medulloblastoma carrying *hTERT* promoter mutations compared with wild-type ones ($n = 76$; Mann-Whitney U-test: $P = 0.03$). (C) Kaplan-Meier curves of overall survival of medulloblastoma patients presenting tumors carrying *hTERT* promoter mutations (red line) compared with wild-type (blue line) ones (log-rank test: $P = 0.34$). (D) Kaplan-Meier curves of overall survival of medulloblastoma patients with tumors having either hypoexpression (red line) or overexpression (blue line) of *hTERT* (log-rank test: $P = 0.72$).

Hotspot *hTERT* somatic mutations have been reported in medulloblastomas with frequencies ranging 4–27%.^{20–22,33,34} In the present study, *hTERT* mutations were observed in 29% of the cases, and these mutations were more frequent in MB_{SHH} as previously described.^{21,22} Moreover, *hTERT* mutations were associated with older-aged patients in accordance with previous studies.^{20,35} Since *hTERT*-activating promoter mutations are reported to enhance telomerase expression,²⁷ we included the *hTERT* gene in the CodeSet of the 22-gene panel for medulloblastoma molecular subgrouping. Unsurprisingly, we observed that *hTERT* mutated cases also exhibited a higher *hTERT* expression.

In the current study, no association was observed between the molecular features (molecular subgroups, *hTERT* mutations status and *hTERT* expression) and OS in the multivariate analysis. Due to the retrospective and multicentric nature of this study, patients were not treated uniformly, which hampers proper outcome analysis.

Our study illustrates the robustness of the NanoString gene expression profiling of FFPE samples, since all 106 cases from different Brazilian institutions provided reliable subgroup classifications. This finding is important because samples from different institutions are likely to have different pre-analytic protocols. Of note, most of the samples in our study had been stored for several years, some of them for more than 20, leading to high levels of nucleic acid degradation, as demonstrated by the difficulties identifying mutational status using traditional analytical methods from the *hTERT* gene for a subset of cases. These findings suggest that molecular profiling of the 22-gene panel will be important for future medulloblastoma clinical trials utilizing RNA from FFPE samples. Importantly, in the revised 2016 WHO CNS classification, a meaningful integration of genetic/biological information with histopathological features is suggested to enable a more precise medulloblastoma classification.²⁶ In this context, the present mRNA-based 22-gene panel accurately

discriminates the four genetically defined medulloblastoma subgroups, which are MB_{WNT}, MB_{SHH} and non-MB_{WNT}/non-MB_{SHH} (MB_{GRP3} and MB_{GRP4}).^{26,36,37} Yet, in the update of WHO classification, the MB_{SHH} subgroup should further divided in accordance with *TP53* status that differentiates two different MB_{SHH} disease entities, displaying distinct genetic features, age of diagnosis and outcome.^{36–38}

Concluding, we successfully implemented the 22-gene panel originally described by Northcott and colleagues for medulloblastoma molecular classification in a multicenter Brazilian cohort of FFPE cases employing the nCounter[®] technology. Our findings demonstrate the feasibility of medulloblastoma molecular subgrouping in a routine clinical testing.

ACKNOWLEDGEMENTS

We thank Barretos Cancer Hospital and FINEP (MCTI/FINEP/MS/SCTIE/DECIT - BioPlat 1302/13) for partially funding the present study. LFL is supported by Public Ministry of Labor Campinas (Research, Prevention and Education of Occupational Cancer) in Campinas, Brazil. RMR is sponsored by National Council for Scientific and Technological Development (CNPq, Brazil).

DISCLOSURE

The authors declare they have nothing to disclose.

REFERENCES

- McNeil DE, Cote TR, Clegg L, Rorke LB. Incidence and trends in pediatric malignancies medulloblastoma/primitive neuroectodermal tumor: A SEER update. *Surveillance epidemiology and end results. Med Pediatr Oncol* 2002; **39**: 190–194.
- Packer RJ, Vezina G. Management of and prognosis with medulloblastoma: Therapy at a crossroads. *Arch Neurol* 2008; **65**: 1419–1424.
- INCA. Instituto Nacional do Câncer - Estimativa 2010: Incidência de câncer no Brasil. 2009 [cited 12 April 2018]. Available from URL: http://www2.inca.gov.br/wps/wcm/connect/agencianoticias/site/home/noticias/2009/lancamento_estimativa_2010.
- Chan AW, Tarbell NJ, Black PM *et al.* Adult medulloblastoma: Prognostic factors and patterns of relapse. *Neurosurgery* 2000; **47**: 623–631; discussion 31–2.
- Ellison DW. Childhood medulloblastoma: Novel approaches to the classification of a heterogeneous disease. *Acta Neuropathol* 2010; **120**: 305–316.
- Taylor RE, Bailey CC, Robinson KJ *et al.* Outcome for patients with metastatic (M2-3) medulloblastoma treated with SIOP/UKCCSG PNET-3 chemotherapy. *Eur J Cancer* 2005; **41**: 727–734.
- Gajjar A, Hernan R, Kocak M *et al.* Clinical, histopathologic, and molecular markers of prognosis: Toward a new disease risk stratification system for medulloblastoma. *J Clin Oncol* 2004; **22**: 984–993.
- Gilbertson RJ, Ellison DW. The origins of medulloblastoma subtypes. *Annu Rev Pathol* 2008; **3**: 341–365.
- Gilbertson R, Wickramasinghe C, Hernan R *et al.* Clinical and molecular stratification of disease risk in medulloblastoma. *Br J Cancer* 2001; **85**: 705–712.
- Kim W, Choy W, Dye J *et al.* The tumor biology and molecular characteristics of medulloblastoma identifying prognostic factors associated with survival outcomes and prognosis. *J Clin Neurosci* 2011; **18**: 886–890.
- de Haas T, Hasselt N, Troost D *et al.* Molecular risk stratification of medulloblastoma patients based on immunohistochemical analysis of MYC, LDHB, and CCNB1 expression. *Clin Cancer Res* 2008; **14**: 4154–4160.
- von Bueren AO, Kortmann RD, von Hoff K *et al.* Treatment of children and adolescents with metastatic medulloblastoma and prognostic relevance of clinical and biologic parameters. *J Clin Oncol* 2016; **34**: 4151–4160.
- Ramaswamy V, Remke M, Bouffet E *et al.* Risk stratification of childhood medulloblastoma in the molecular era: The current consensus. *Acta Neuropathol* 2016; **131**: 821–831.
- Thompson MC, Fuller C, Hogg TL *et al.* Genomics identifies medulloblastoma subgroups that are enriched for specific genetic alterations. *J Clin Oncol* 2006; **24**: 1924–1931.
- Kool M, Koster J, Bunt J *et al.* Integrated genomics identifies five medulloblastoma subtypes with distinct genetic profiles, pathway signatures and clinicopathological features. *PLoS One* 2008; **3**: e3088.
- Northcott PA, Korshunov A, Witt H *et al.* Medulloblastoma comprises four distinct molecular variants. *J Clin Oncol* 2011; **29**: 1408–1414.
- Taylor MD, Northcott PA, Korshunov A *et al.* Molecular subgroups of medulloblastoma: The current consensus. *Acta Neuropathol* 2012; **123**: 465–472.
- Kool M, Korshunov A, Remke M *et al.* Molecular subgroups of medulloblastoma: An international meta-analysis of transcriptome, genetic aberrations, and clinical data of WNT, SHH, Group 3, and Group 4 medulloblastomas. *Acta Neuropathol* 2012; **123**: 473–484.
- Remke M, Hielscher T, Northcott PA *et al.* Adult medulloblastoma comprises three major molecular variants. *J Clin Oncol* 2011; **29**: 2717–2723.
- Viana-Pereira M, Almeida GC, Stavale JN *et al.* Study of hTERT and histone 3 mutations in medulloblastoma. *Pathobiology* 2017; **84**: 108–113.

21. Remke M, Ramaswamy V, Peacock J *et al.* TERT promoter mutations are highly recurrent in SHH subgroup medulloblastoma. *Acta Neuropathol* 2013; **126**: 917–929.
22. Lindsey JC, Schwalbe EC, Potluri S, Bailey S, Williamson D, Clifford SC. TERT promoter mutation and aberrant hypermethylation are associated with elevated expression in medulloblastoma and characterise the majority of non-infant SHH subgroup tumours. *Acta Neuropathol* 2014; **127**: 307–309.
23. Geiss GK, Bumgarner RE, Birditt B *et al.* Direct multiplexed measurement of gene expression with color-coded probe pairs. *Nat Biotechnol* 2008; **26**: 317–325.
24. Veldman-Jones MH, Brant R, Rooney C *et al.* Evaluating robustness and sensitivity of the NanoString technologies nCounter platform to enable multiplexed gene expression analysis of clinical samples. *Cancer Res* 2015; **75**: 2587–2593.
25. Northcott PA, Shih DJ, Remke M *et al.* Rapid, reliable, and reproducible molecular sub-grouping of clinical medulloblastoma samples. *Acta Neuropathol* 2012; **123**: 615–626.
26. Louis DN, Perry A, Reifenberger G *et al.* The 2016 World Health Organization classification of tumors of the central nervous system: A summary. *Acta Neuropathol* 2016; **131**: 803–820.
27. Batista R, Cruvinel-Carlioni A, Vinagre J *et al.* The prognostic impact of TERT promoter mutations in glioblastomas is modified by the rs2853669 single nucleotide polymorphism. *Int J Cancer* 2016; **139**: 414–423.
28. Waggott D, Chu K, Yin S, Wouters BG, Liu FF, Boutros PC. NanoStringNorm: An extensible R package for the pre-processing of NanoString mRNA and miRNA data. *Bioinformatics* 2012; **28**: 1546–1548.
29. Tibshirani R, Hastie T, Narasimhan B, Chu G. Diagnosis of multiple cancer types by shrunken centroids of gene expression. *Proc Natl Acad Sci U S A* 2002; **99**: 6567–6572.
30. Cho YJ, Tsherniak A, Tamayo P *et al.* Integrative genomic analysis of medulloblastoma identifies a molecular subgroup that drives poor clinical outcome. *J Clin Oncol* 2011; **29**: 1424–1430.
31. Thompson EM, Hielscher T, Bouffet E *et al.* Prognostic value of medulloblastoma extent of resection after accounting for molecular subgroup: A retrospective integrated clinical and molecular analysis. *Lancet Oncol* 2016; **17**: 484–495.
32. Wang X, Dubuc AM, Ramaswamy V *et al.* Medulloblastoma subgroups remain stable across primary and metastatic compartments. *Acta Neuropathol* 2015; **129**: 449–457.
33. Killela PJ, Reitman ZJ, Jiao Y *et al.* TERT promoter mutations occur frequently in gliomas and a subset of tumors derived from cells with low rates of self-renewal. *Proc Natl Acad Sci U S A* 2013; **110**: 6021–6026.
34. Schwalbe EC, Lindsey JC, Nakjang S *et al.* Novel molecular subgroups for clinical classification and outcome prediction in childhood medulloblastoma: A cohort study. *Lancet Oncol* 2017; **18**: 958–971.
35. Koelsche C, Sahm F, Capper D *et al.* Distribution of TERT promoter mutations in pediatric and adult tumors of the nervous system. *Acta Neuropathol* 2013; **126**: 907–915.
36. Pietsch T, Haberler C. Update on the integrated histopathological and genetic classification of medulloblastoma - A practical diagnostic guideline. *Clin Neuropathol* 2016; **35**: 344–352.
37. Louis D, Ohgaki H, Wiestler O, Cavenee W. *WHO Classification of Tumours of the Central Nervous System*, 4th edn. Lyon, France: International Agency for Research on Cancer, 2016. 408 p.
38. Zhukova N, Ramaswamy V, Remke M *et al.* Subgroup-specific prognostic implications of TP53 mutation in medulloblastoma. *J Clin Oncol* 2013; **31**: 2927–2935.

SUPPORTING INFORMATION

Additional supporting information may be found in the online version of this article at the publisher's website: <http://onlinelibrary.wiley.com/doi/supinfo>.

Table S1 Clinical, pathological and molecular characteristics and outcomes of the Brazilian series of medulloblastomas analyzed in the present study.

Table S2 Univariate analysis of disease-specific overall survival associated with clinical, pathological and molecular characteristics of the Brazilian series of medulloblastomas.

Figure S1 Heatmap clustering of Canadian series ($n = 240$) class prediction control dataset combined with the Brazilian cohort series ($n = 104$). On the top and on the right side, each colored column represents a medulloblastoma subgroup: MB_{SHH}, red; MB_{WNT}, blue; MB_{GRP4}, purple; MB_{GRP3}, green. Lower right square: gene expression scaling from dark red to dark blue; red, increased gene expression; blue, decreased gene expression (as described in legend to Fig. 1).